Competitive Photoelectrochemical Oxidation of Reducing Agents at the TiO_2 Photoanode

Akira Fujishima,* Tooru Inoue, and Kenichi Honda

Contribution from the Department of Synthetic Chemistry, Faculty of Engineering, The University of Tokyo, Hongo, Bunkyo-ku, Tokyo 113, Japan.

Received September 22, 1978

Abstract: Competitive photoelectrochemical oxidation of a variety of reducing agents at the TiO_2 single crystal photoanode was investigated by means of the rotating ring-disk electrode technique. The competitive oxidation phenomena can be elucidated based on the redox potentials of electroactive species. A reducing agent with a more negative redox potential is oxidized in preference to others. Both the pH dependence of competitive oxidation and stability of the TiO_2 photoanode are explained, based on charge transfer with participation of the surface states, focusing upon the redox potentials.

When a semiconductor is irradiated with absorbable light at the band gap frequency (3.0 eV for TiO_2) electrons are promoted from the valence band to the conduction band. Positively charged holes remain in the valence band and a few electrons occupy the conduction band. Because the holes in the valence band can accept electrons, an appropriately irradiated electrode can serve as an effective oxidizing agent to release O_2 from a water solution.[1,2] The equation describing such a process for an illuminated TiO_2 electrode is

$$2H_2O + 4(\text{electrode holes})^+ \xrightarrow[h\nu \text{ at } 415 \text{ nm}]{TiO_2} O_2 + 4H^+ \qquad (1)$$

Figure 1 presents a schematic representation of the above process. Other substances besides water may also be photooxidized. The generalized equations are

$$\underset{\text{form}}{\text{reduced}} + \text{hole}^+ \rightarrow \underset{\text{form}}{\text{oxidized}} \qquad (2)$$

This photoelectrochemical process at the semiconductor-solution junction has given rise to the electrochemical photocell as a solar energy conversion device.[1-12] In some case the holes result in electrode disintegration rather than oxidation of water or another species.[13-21] To minimize this undesirable electrode disintegration, the processes for CdS, CdSe, CdTe, and Bi_2S_3 electrodes have been studied. Some electrode stabilization has been achieved by adding reducing agents to the electrolyte solution[22,23] or by coating the electrode with a stabilizing film.[31-34]

In the present study, we have investigated the photoelectrochemical competitive oxidation of a variety of reducing agents introduced into the electrolyte solution by the action of photogenerated holes at the TiO_2 photoanode. Results of the competitive oxidation were interpreted on the basis of the charge transfer across the semiconductor electrode-solution interface with participation of the surface states, focusing upon the redox potentials of the electroactive species.

The rotating ring-disk electrode (RRDE) technique served as a useful tool for the in situ determination of the relative competitive oxidation reactivities of the redox agents.

Experimental Section

The TiO_2 single crystal (Nakazumi Crystal Co. Ltd., n-type, *c*-axis cut) employed in the present study was reduced in a H_2 atmosphere at 500 °C for 15 min. The crystal was shaped into a disk 6.0 mm in diameter and 1.0 mm in thickness. Indium was vacuum evaporated onto one face of the crystal in order to ensure an ohmic contact with the conducting wire. Then the TiO_2 disk was mounted on a Teflon rod using epoxy resin together with a Pt ring 7.0 mm in inner diameter and 9.0 mm in outer diameter, thus producing a ring-disk electrode system. The crystal face of TiO_2 exposed to the electrolyte solution was polished with alumina powder, etched in concentrated H_2SO_4 for 10 s, and then washed with water. The cell was constructed of Pyrex glass with a quartz window installed at the bottom for illumination and with a Pt counterelectrode. The ring-disk electrode thus prepared was connected into an RRDE measurement system (Nikko Keisoku), which has been described elsewhere.[22,35,36] The potentials of the disk and ring electrodes were controlled independently by means of a dual potentiogalvanostat (Nikko Keisoku). The light source was a 500-W high-pressure mercury arc lamp and the wavelength of the illuminating light was selected with a UV-D2 (Toshiba Kasei) glass filter which passes the wavelengths from 300 to 400 nm. The TiO_2-electrolyte interface was uniformly illuminated through the quartz window. The supporting electrolyte was 0.2 M Na_2SO_4 and all redox agents used were reagent grade. In most of the RRDE experiments, the potential of the TiO_2 disk electrode was kept at 1.0 V vs. SCE where a saturation photocurrent occurred, and the potential of the Pt ring electrode was swept at a rate of 30 s/V in order to analyze the products of the photoelectrochemical reaction on the TiO_2 disk electrode. The rotational speed of the RRDE was set at 1000 rpm. All solutions were deaerated with highly purified nitrogen for each experiment.

The measurement principle of the RRDE method is schematically illustrated in Figure 2. In the absence of a reducing agent (Red) in the electrolyte solution (A), oxygen gas is produced at the disk electrode through the photoelectrochemical process (1), and of that oxygen a portion, determined by the collection efficiency, is reduced at the Pt ring electrode. If a reducing agent (Red) is added (B), it undergoes competitive oxidation (2) by photogenerated holes, and the oxidized species (O_x) discharges at the ring electrode.

Results and Discussion

1. Competitive Oxidation of Halides at the TiO_2 Photoanode.

Figure 3A shows the currents at the TiO_2 disk and Pt ring electrodes in 0.2 M Na_2SO_4 aqueous solution as a function of the ring potential with and without illumination. I_D, I_R, E_D, and E_R denote the disk current, the ring current, the disk potential, and the ring potential, respectively. In darkness, the TiO_2 disk current is negligibly small at the fixed potential of 1.0 V vs. SCE; hydrogen evolution occurs at potentials more negative than −0.5 V vs. SCE and oxygen evolution at potentials more positive than +0.9 V vs. SCE at the Pt ring electrode. Under illumination a constant anodic photocurrent flows at the TiO_2 disk electrode; the current is controlled by the diffusion of the excess holes in proportion to the incident photons at the electrode surface and independent of the rotational speed of the RRDE. At the same time, a reduction current appears at the Pt ring electrode in the potential range more negative than ca. 0.1 V vs. SCE, which corresponds to the reduction of the oxygen and the small quantity of H_2O_2[37] generated at the illuminated TiO_2 disk electrode.

Figure 3B shows the Pt-TiO_2 RRDE currents as a function of the disk potential with and without illumination, where the Pt ring electrode was polarized at −0.2 V vs. SCE to detect the oxygen. The reduction current for oxygen at the Pt ring elec-

0002-7863/79/1501-5582$01.00/0

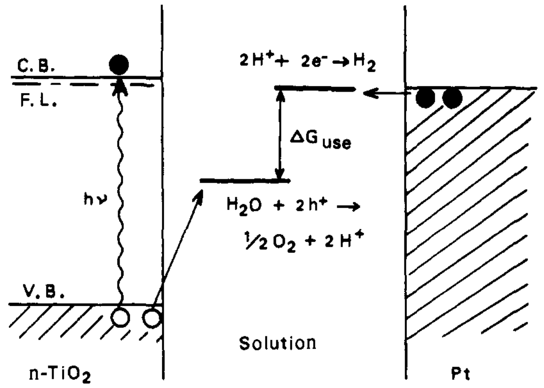

Figure 1. Schematic explanation of photoelectrochemical decomposition of water in the semiconductor photoelectrode-solution junction photocell.

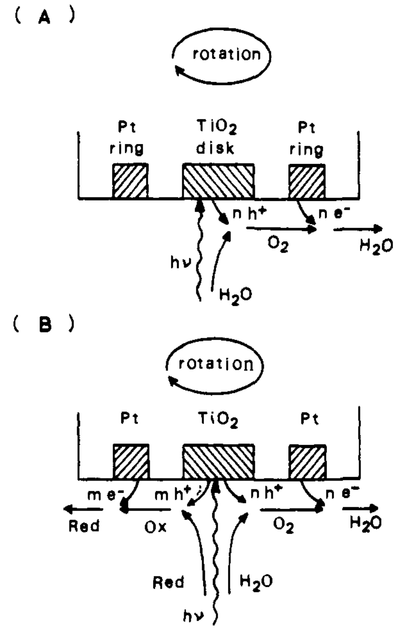

Figure 2. Schematic illustration for detection of photoanodic products at the TiO_2 disk electrode by means of RRDE measurements. (A) Detection of oxygen produced at TiO_2 in the absence of reducing agents in the solution. (B) Detection of oxygen and oxidized species produced at TiO_2 in the presence of a reducing agent in the solution.

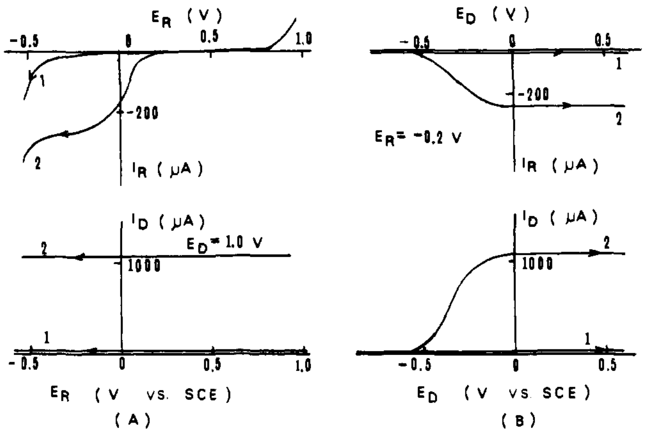

Figure 3. Current-potential curves (I_R-E_R, I_D-E_R; I_R-E_D, I_D-E_D) at the Pt-TiO_2 RRDE in the supporting electrolyte (0.2 M Na_2SO_4) solution. The rotational speed of the RRDE was controlled at 1000 rpm. (A) The potential (E_D) of the TiO_2 disk electrode was fixed at 1.0 V vs. SCE, and the potential (E_R) of the Pt ring electrode was swept. Curve 1, in the dark; curve 2, under illumination. (B) Potential of the Pt ring electrode was fixed at −0.2 V vs. SCE, and that of the TiO_2 disk electrode was swept. Curve 1, in the dark; curve 2, under illumination.

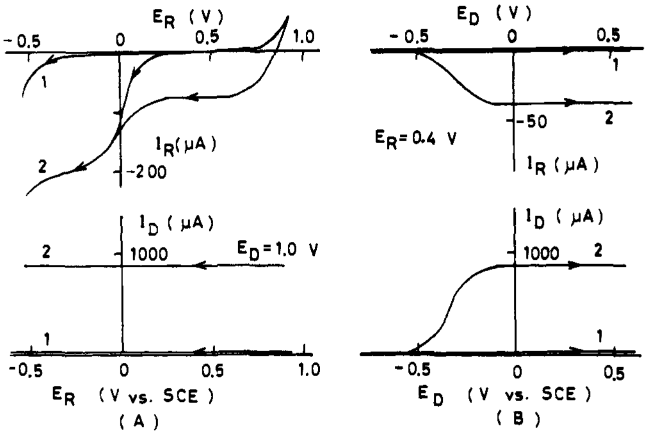

Figure 4. Current-potential curves at the Pt-TiO_2 RRDE in the aqueous electrolyte (0.2 M Na_2SO_4 + 0.1 M KBr) solution. (A) E_D was fixed at 1.0 V vs. SCE, and E_R was swept. Curve 1, in the dark; curve 2, under illumination. (B) E_R was fixed at 0.4 V vs. SCE, and E_D was swept. Curve 1, in the dark; curve 2, under illumination.

trode appears at the same time as the appearance of the anodic photocurrent at the TiO_2 disk electrode. Therefore, we can appreciate that oxygen arises under the condition of positive polarization with respect to the flatband potential of the TiO_2 electrode under illumination. The quantum yield of electrolysis is ca. 0.9.

The current-potential characteristics of Pt-TiO_2 RRDE measurements in the case of addition of halide anions (X^-: I^-, Br^-, Cl^-) to the electrolyte solution were obtained and that for the case of Br^- is shown in Figure 4. In the current-potential curves (I_R-E_R, I_D-E_R curves) in Figure 4A, the magnitude of the disk photocurrent undergoes practically no change in comparison with the case in Figure 3A. The ring current (I_R) for the reduction of halogen (Br_2) appears at a potential more negative than the redox potential of the Br^-/Br_2 system. Similar results were obtained for the cases of I^- and Cl^-. These results show that, besides water, halide anions are oxidized at the illuminated TiO_2 electrode.

$$2X^- + 2h^+ \rightarrow X_2 \qquad (3)$$
$$(X\text{: I, Br, and Cl})$$

Under the conditions of polarization of the Pt ring electrode allowing detection of the reduction of halogens and oxygen, the cathodic reduction currents of halogens and oxygen at the ring electrode appear at the same time that the anodic photocurrents appear at the TiO_2 electrode at a potential more positive than the flatband potential. For the case of Br^-, current-potential curves were obtained as a function of the disk electrode potential with and without Br^- under illumination as shown in Figure 4B. Therefore, halide anions also undergo photosensitized electrolytic oxidation at the TiO_2 electrode because these oxidation potentials of halide anions are more positive than the flatband potential and more negative than the oxidation potentials at usual metal electrodes. Therefore, the photoanodic reactions proceed on the illuminated TiO_2 electrode with competition between processes 1 and 3.

From the RRDE measurements, we can obtain individual values for the oxidation efficiencies of reducing agents such as halide anions and water by calculating the ring current for reduction of oxidized products generated at the illuminated TiO_2 electrode. In what follows, the cathodic limiting current at the ring electrode corresponding to the reduction of halogen

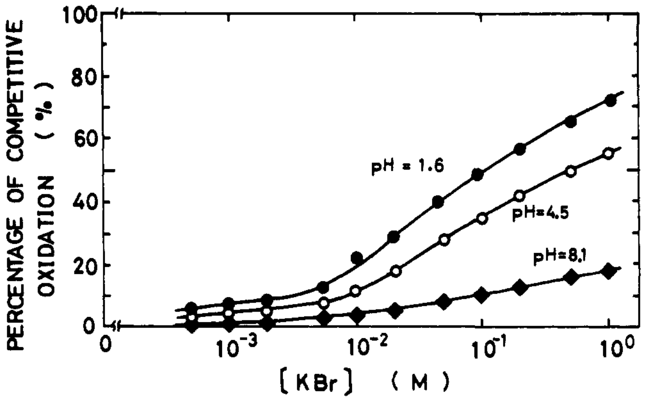

Figure 5. Dependence of the percentage of competitive oxidation of Br^- against water on its concentration and the pH in the electrolyte solution.

(X_2: I_2, Br_2, and Cl_2) is expressed as I_R for the electrolyte solution containing a redox agent (X^-), and as $I_R{}^0$ for the reduction of oxygen in the solution not containing the reducing agent. Without a halide anion in the electrolyte solution, it is found that the ratio of the magnitude of $I_R{}^0$ to that of the anodic photocurrent at the TiO_2 disk electrode coincides fairly well with the theoretical collection efficiency[36,37] for the RRDE employed in this study. This implies that in this case the ring current $I_R{}^0$ due to process 1 is totally responsible for the anodic photocurrent. From this it follows that the value of $I_R/I_R{}^0$ or $(I_R{}^0 - I_R)/I_R{}^0$ represents the fraction of the anodic photocurrent based on the process 1 or 3, respectively. We call η the percentage of competitive oxidation expressed by the equations

$$\eta_1 = 100 I_R/I_R{}^0 \quad (\%) \tag{4}$$

$$\eta_2 = 100(I_R{}^0 - I_R)/I_R{}^0 \quad (\%) \tag{5}$$

$$\eta_1 + \eta_2 = 100 \quad (\%) \tag{6}$$

where η_1 and η_2 correspond to the percentages of photoanodic reactions 1 and 3 at the illuminated TiO_2 electrode, respectively.

2. Dependence of Competitive Oxidation on Concentration. The percentages of competitive oxidation of halide anions were obtained as a function of their concentrations in the electrolyte solution at the various pH values where the percentage of competitive oxidation of water was expressed by the value $(100 - \eta)$. The competitive oxidation percentage for halide anions increases with increasing concentration of the redox agents (X^-) and decreases with increasing electrolyte solution pH, and reaches values of nearly 100% under conditions of low pH and high halide anion concentration in the electrolyte solution. Figure 5 shows the result for the case of Br^-. The concentration and pH dependences of the percentages of competitive oxidation have the same general tendency for each of these three halide anions. However, the magnitude of the competition percentage followed the sequence $I^- > Br^- > Cl^-$ for the comparable concentrations and pH. Moreover, the percentage of the competitive oxidation with fixed conditions of concentration of the redox agents and pH remains constant vs. the intensity of irradiation of the TiO_2 electrode and the rotational speed of the ring-disk electrode device shown in Figure 6. This result suggests that the halide anions exist in large quantities on the TiO_2 electrode surface and the anodic photocurrent is controlled by the diffusion of photogenerated holes in the space charge layer.

Therefore, regarding the concentration dependence of the percentage of the competitive oxidation, the following mechanism which includes adsorption processes is proposed: first, holes and electrons are generated in the valence band and conduction band, respectively, by the irradiation of TiO_2 at a wavelength shorter than the absorption threshold.

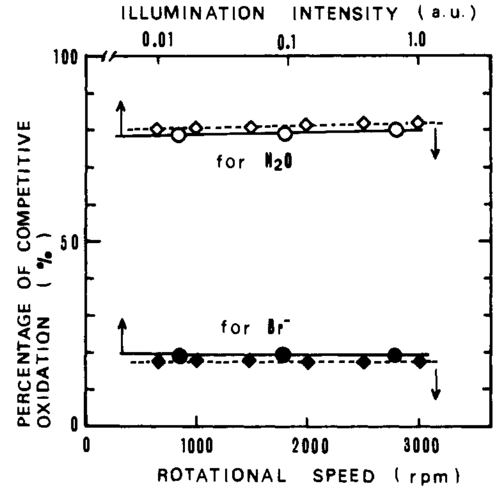

Figure 6. Dependence of the percentage of competitive oxidation on the illumination intensity and the RRDE rotational speed.

$$TiO_2 + h\nu \xrightarrow{k_1} TiO_2{}^*(h^+{}_{val} + e^-{}_{cond}) \tag{7}$$

Then these photogenerated carriers are separated by the electric field in the space charge layer and in the next stage the holes at the electrode surface are consumed by the following reactions:

$$h^+{}_{val} + e^-{}_{cond} \xrightarrow{k_2} \text{heat} \tag{8}$$

$$h^+{}_{val} + \text{trap} \xrightarrow{k_3} \text{trap}^+ \tag{9}$$

$$h^+{}_{val} + {}^1\!/_2H_2O^* \xrightarrow{k_4} {}^1\!/_4O_2 + H^+ \tag{10}$$

$$h^+{}_{val} + X^{-*} \xrightarrow{k_5} {}^1\!/_2X_2 \tag{11}$$

where trap denotes the trap state, H_2O^* and X^{-*} the adsorbed species, and k_i the reaction rate constant. Hence, the current I_1 corresponding to the oxidation of water by the photogenerated holes is appxoximately expressed by the equations

$$\frac{I_1}{F} = \frac{K_1Q}{K_2 + k_4[H_2O^*] + k_5[X^{-*}]} k_4[H_2O^*] \tag{12}$$

$$K_1 = k_1A, \quad K_2 = k_2[e^-] + k_3\,\text{trap} \tag{13}$$

where Q denotes the quantity of the absorbed photons, F the Faraday constant, A the area of the electrode surface, and the brackets the concentrations of active species. The equations in (13) are adopted in a steady state. Also the current I_2 corresponding to the oxidation of the halide anion is expressed as follows:

$$\frac{I_2}{F} = \frac{K_1Q}{K_2 + k_4[H_2O^*] + k_5[X^{-*}]} k_5[X^{-*}] \tag{14}$$

Since the anodic photocurrent I_D at the TiO_2 disk electrode is the sum of I_1 and I_2, the following equations are obtained:

$$\frac{I_1 + I_2}{F} = \frac{I_D}{F} = \frac{K_1(k_4[H_2O^*] + k_5[X^{-*}])}{K_1 + k_4[H_2O^*] + k_5[X^{-*}]} Q \tag{15}$$

Since it was found that the anodic photocurrent at the TiO_2 disk electrode is proportional to the light intensity but independent of the concentration of the halide anion, the following

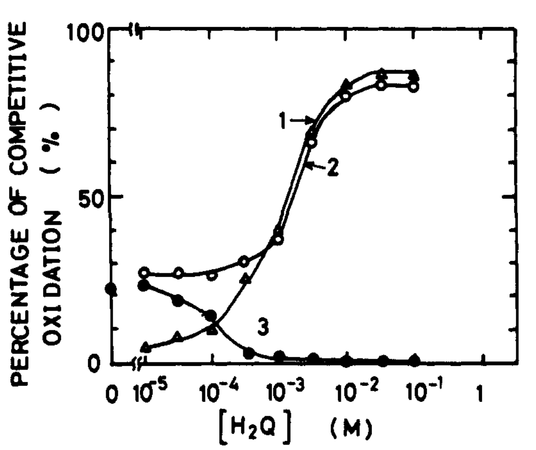

Figure 7. Dependence of percentages of competitive oxidation on H_2Q concentration in the mixed system of H_2Q, KCl, and water. Curve 1, dependence of the percentage of competitive oxidation of H_2Q on its concentration in absence of Cl^- in the solution; curve 2, dependence of the percentage of competitive oxidation of H_2Q and Cl^- on H_2Q concentration, with a fixed concentration of 0.01 M Cl^-; curve 3, dependence of the percentage of competitive oxidation of Cl^- alone on H_2Q concentration, with a fixed concentration of 0.01 M Cl^-.

equation can be obtained:

$$\frac{I_D/F}{Q} = \frac{K_1(k_4[H_2O^*] + k_5[X^{-*}])}{K_2 + (k_4[H_2O^*] + k_5[X^{-*}])} \sim K_1 \qquad (16)$$

where the following condition must be satisfied at a well prepared TiO_2 electrode:

$$k_4[H_2O^*] + k_5[X^{-*}] \gg K_2 \qquad (17)$$

Therefore, by combining eq 14 and 16, the following expression for the competitive oxidation percentages (η_1 and η_2) can be obtained:

$$\frac{\eta_1}{100} = \frac{I_2}{I_D} = \frac{k_5[X^{-*}]}{k_4[H_2O^*] + k_5[X^{-*}]} \qquad (18)$$

and

$$\frac{\eta_2}{100} = \frac{I_1}{I_D} = \frac{k_4[H_2O^*]}{k_4[H_2O^*] + k_5[X^{-*}]} \qquad (19)$$

Next, it is supposed that the percentages of competitive oxidation of water and halide anions depend upon the surface concentration of their adsorbed species on the TiO_2 electrode surface and the rate constants of charge transfer across the interface at the TiO_2 electrode-electrolyte solution junction. At this point, the characteristics of an adsorption equilibrium must be taken into account because the surface concentrations of the reducing agents are related to their concentration in the bulk electrolyte solution. It is felt that further investigations on the adsorption isotherm will be necessary for a detailed interpretation of the competitive oxidation.

3. Dependence of Competitive Oxidation on pH Variation. As for the effect of variation in the pH of the electrolyte solution on the competitive oxidation between halide anions and water in Figure 5, the following elucidation is possible on the basis of the pH-potential relationship (Pourbaix diagram[38]) for the redox couples H_2O/O_2 and X^-/X_2 and of the pH variation of the flatband potential of the TiO_2 electrode. Both the redox potential of couple H_2O/O_2 and the flatband potential of the TiO_2 electrode decrease with pH by −59 mV/pH unit.[39,40] On the contrary, the redox potentials of the couple X^-/X_2 are constant against pH in the range of the acidic and neutral media. From the standpoint of potential characteristics, the oxidation reactivity of water increases with an increase in pH, whereas those of halide anions remain constant. Therefore, it is supposed that the effect of the oxidation reactivity on the potential characteristics can explain the pH dependence of the competitive oxidation at the TiO_2 photoanode.

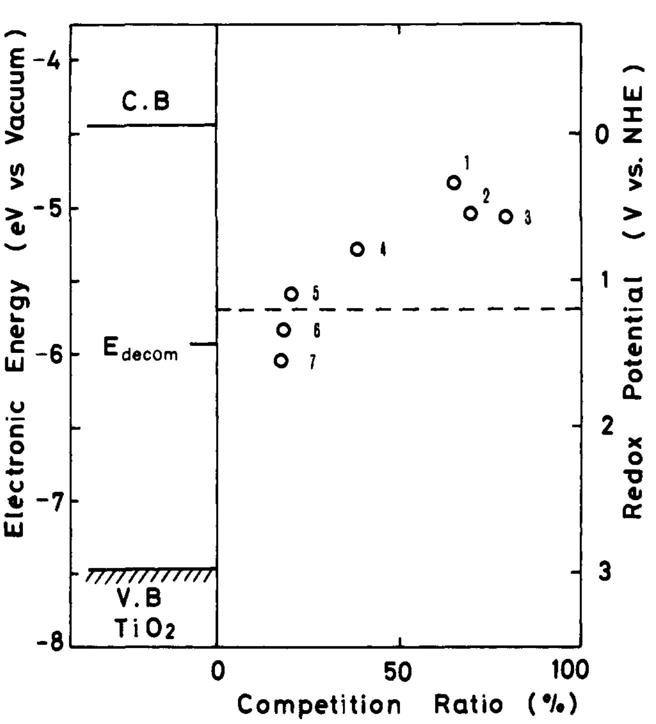

Figure 8. Percentages of competitive oxidation of various reducing agents (0.01 M) as a function of their redox potentials. E_{decom} denotes the oxidative decomposition potential of TiO_2. Supporting electrolyte solution is 0.5 M H_2SO_4. 1, $Fe(CN)_6^{3-/4-}$; 2, I_2/I^-; 3, Q/H_2Q; 4 $Fe^{3+/2+}$; 5, Br_2/Br^-; 6, Cl_2/Cl^-; 7, $Mn^{3+/2+}$.

4. Competitive Oxidation in Mixed System. In order to investigate competitive oxidation between minority agents, we added two kinds of reducing agents to the same electrolyte solution. Each of the two reducing agents was able to be photoelectrochemically oxidized with the oxygen evolution (1). Figure 7 shows the percentage of competitive oxidation for a hydroquinone-Cl^- mixed system as a function of hydroquinone (H_2Q) concentration in 0.5 M aqueous H_2SO_4 solution. Curve 1 corresponds to the case where only hydroquinone is present in the electrolyte solution, while curve 2 shows the total effect for the hydroquinone-Cl^- mixture, with the fixed concentration of 0.01 M Cl^-. Curve 3 corresponds to the percentage of competitive oxidation of Cl^- alone in the mixed system. For the results shown in Figure 7 one can estimate the effectiveness of photosensitized oxidation of each reducing agent at the TiO_2 photoanode under particular conditions. For example the percentage of the competitive oxidation of H_2O:Cl^-:hydroquinone, at concentrations of 56, 0.01, and 0.0001 M, respectively, is approximately 73:15:12. Further, the ratio of the oxidizability of Cl^- to that of hydroquinone, at a common concentration of 0.01 M, is nearly 1:50.

This result suggests that the competitive oxidation of the reducing agents by holes may bear a general relationship to the redox potentials of the reducing agents; that is, the reducing agent with the more negative redox potential may by photoelectrochemically oxidized in preference to other reducing agents.

5. Competitive Oxidation of Various Reducing Agents. Figure 8 summarizes the percentages of competitive oxidation for a variety of reducing agents as a function of their redox potentials vs. NHE, referring to the energy levels of the TiO_2 electrode. Each reducing agent was employed at the concentration of 0.01 M. These results can be considered to agree with the above hypothesis of a dependence of the percentage of competitive oxidation on the redox potential of reducing agents,

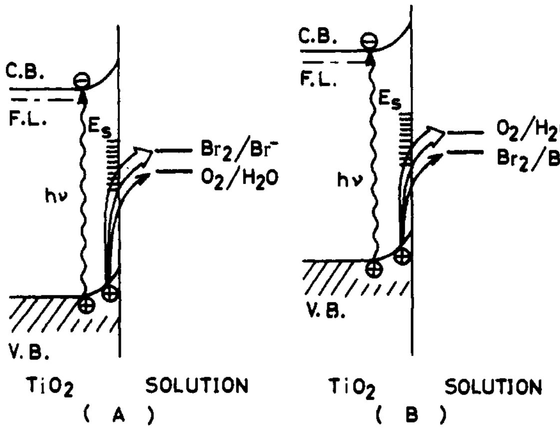

Figure 9. Schematic explanation of the efficiency of oxidation between Br^- and water. E_s denotes the surface states: (A) in an acidic aqueous solution; (B) in a neutral and a basic aqueous solution.

and findings similar to ours have been presented elsewhere by Frank and Bard.[41] As for CdS, ZnO, and GaP photoanodes, the competitive oxidation characteristics at these photoelectrodes have been investigated in terms of the redox potentials of reducing agents and have been presented by ourselves, as well as by other authors.[22,24,25,42] Unstable photoelectrodes such as CdS, ZnO, and GaP were stabilized through the competitive reaction of redox agents in the electrolyte solution.

6. Hole Transfer across the Interface of the TiO_2 Photoanode–Electrolyte Solution Junction. Semiconductor electrodes are peculiar electrodes because they possess two kinds of bands (a conduction and a valence band) and the space charge layer at their surfaces. The energy levels of band edges of semiconductor electrodes are determined by the physical and/or chemical characteristics of the system; in particular, the position of the flatband potential (E_{fb}) of the TiO_2 electrode is determined mainly by pH in the solution. Electron-hole pairs generated by the incident photons are separated by the electric field in the space charge layer; then holes as minority carriers are consumed by the electrochemically active species at the interface. As for the hole transfer mechanism, according to Gerischer,[43] the transfer rate is determined from the overlap of the relative distribution of states in the valence band and the redox agents in the electrolyte solution, that is

$$I_{OX} = k^0[\mathrm{Red}] \int_{-\infty}^{0} K^0(E) D_+(E) W_R(E) \mathrm{d}E \qquad (20)$$

where I_{OX} is the anodic photocurrent, [Red] is the concentration of reducing agents in the solution, $D_+(E)$ is the density of photogenerated holes in the semiconductor, and $W_R(E)$ is the distribution function of reducing agent in the solution. As the distribution of $Fe(CN)_6{}^{4-}$, for example, locates within the band gap of TiO_2,[44] it is expected from a conceptual model of point charges that it will be difficult for $Fe(CN)_6{}^{4-}$ to be oxidized by the photogenerated holes in the valence band whereas $Fe(CN)_6{}^{3-}$ will be reduced by the electrons in the conduction band. However, $Fe(CN)_6{}^{4-}$ is actually oxidized well by the photogenerated holes at the TiO_2 photoelectrode as shown in Figure 8.

Therefore, we can suggest another mechanism of hole transfer for the oxidation of reducing agents. Intermediate surface states have been mentioned for the TiO_2 electrode by some investigators.[16,41,45] For the case with participation of surface states, we can rewrite eq 20 as the summation of matrices as

$$\begin{aligned} I_{OX} = k^0[\mathrm{Red}]\{&\langle D_+(E_s)|\mathbf{K}(E_s)|W_R(E_s)\rangle \\ &+ \langle D_+(E_{VB})|\mathbf{K}(E_{VB})|W_R(E_{VB})\rangle\} \qquad (21) \end{aligned}$$

where E_s and E_{VB} represent the energy of surface states and the energy of the valence band edge, respectively, $\langle\ \rangle$ denotes averaging over sites, and **K** represents the collision function. The total photocurrent at the TiO_2 electrode is a summation of I_{OX} terms of the individual reducing agents. We can express the percentage of competitive oxidation as

$$\begin{aligned} \frac{\eta_i}{100} = k_i{}^0[\mathrm{Red}]_i\{&\langle D_+(E_s)|\mathbf{K}_i(E_s)|W_{R_i}(E_s)\rangle \\ &+ \langle D_+(E_{VB})|\mathbf{K}(E_{VB})|W_{R_i}(E_{VB})\rangle\} \Big/ \sum_i k_i{}^0[\mathrm{Red}]_i \\ &\times \{\langle D_+(E_s)|\mathbf{K}_i(E_s)|W_{R_i}(E_s)\rangle \\ &+ \langle D_+(E_{VB})|\mathbf{K}_i(E_{VB})|W_{R_i}(E_{VB})\rangle\} \qquad (22) \end{aligned}$$

If all holes transfer to reducing agents via the surface states, we can neglect the term $\langle D_+(E_{VB})|\mathbf{K}_i(E_{VB})|W_{R_i}(E_{VB})\rangle$, when the density of surface states largely determines the charge transfer across the interface.

As for the hole transfer, for example, in the combination of water and Br^- in the solution with different pH values, the elucidation of competitive efficiency of oxidation can be schematically illustrated in Figure 9, where holes transfer occurs via the surface states. Frank and Bard have reported that the position of the surface states is 1.6 eV below the conduction band.[16] Yazawa et al. have reported band-like surface states within the TiO_2 band gap.[45] Perhaps the surface states can be created by an adsorption of reducing agents in a solution as well as by dislocations in the crystal surface and the treatment of the electrode.

The redox potentials of Br^-/Br_2 and H_2O/O_2 are located near the surface states, so that the energy distribution of Br^- and H_2O can overlap with that of the surface states. At the lower pH values (Figure 9A) the redox potential of Br^-/Br_2 is more negative than that of H_2O/O_2, so that the overlap of the distribution of Br^- with that of surface states is larger than the overlap of H_2O distribution with that of surface states. On the other hand, at higher pH (Figure 9B) the redox potential of H_2O/O_2 becomes more negative than that of Br^-/Br_2, so that the overlap of the H_2O distribution with the distribution of surface states increases in comparison with the case at lower pH; thus the percentage of competitive oxidation of H_2O becomes larger than that of Br^- with an increase in pH.

The dependence of the competitive oxidation of reducing agents on the redox potentials can be explained by reasoning in the same manner as above.

7. Stability of TiO_2 Photoanode. In general, the redox reactivity of electroactive species depends on the redox potential. TiO_2 itself is also an electroactive species besides the redox agents employed in this study. The oxidation potential E_{decom} of TiO_2 was derived from thermodynamic data based on the following electrochemical decomposition process:[46]

$$TiO_2 \rightleftharpoons TiO^{2+} + {}^1\!/\!_2 O_2 + 2e^- \qquad (23)$$

$$E_{decom} = 1.42 \text{ V (vs. NHE, pH 0)} \qquad (24)$$

The decomposition potential E_{decom} of TiO_2 is more positive than the oxidation potential of water in all ranges of pH values.

As for unstable photoelectrodes such as CdS and ZnO, their oxidation potentials are more negative than that of water as reported by Bard and Wrighton.[46] In earlier reports,[22,25,42] we stabilized these unstable photoanodes through the competitive reaction of reducing agents whose redox potentials are negative with respect to the oxidation potentials of the unstable photoelectrodes.

Decomposing oxidation of TiO_2 can compete with oxidation of water with respect to the action of photogenerated holes. However, from the situation that the redox potential of water

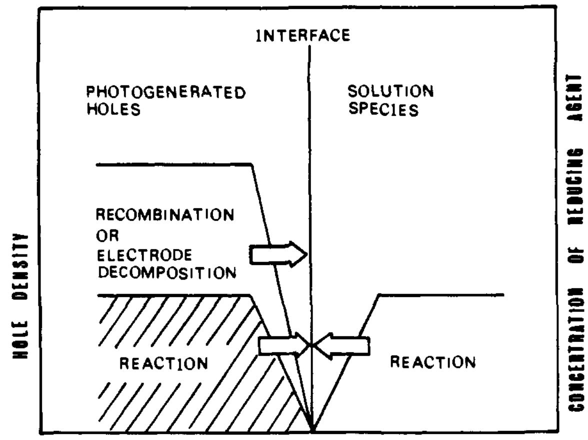

Figure 10. Schematic profile of the relative numbers of photogenerated holes and reducing agents at the interface. The hatched part denotes the number of holes with the ability to oxidize reducing agents in the solution.

is more negative than that of TiO_2 and the concentration of water in a solution is greatly in excess (56 M), the competitive oxidation of water predominates over the oxidation of TiO_2 itself because the overlap of the energy distribution of water with the surface states is much greater than that of TiO_2. This is the reason why the TiO_2 photoanode is a stable photeoelectrode. Bard and Wrighton,[46] as well as Gerischer,[47] have discussed the stability of the semiconductor photoelectrodes from thermodynamic points of view, and our results in this paper coincide well with their findings.

As for reducing agents, one reducing agent can compete with other reducing agents in being oxidized by holes created by incident photons. Water is also a reducing agent present in a major amount in an aqueous solution. Therefore, we can suppose that, when the concentration of water in a solution is relatively small in comparison to the number of photogenerated holes at the electrode surface, the holes remaining after some are consumed in water oxidation can oxidize other electroactive species such as supporting electrolytes and the electrode per se, or can recombine with electrons in the conduction band. Actually, the supporting electrolytes such as SO_4^{2-} (the redox potential of $SO_4^{2-}/S_2O_8^{2-}$ is nearly 2.0 V vs. NHE) were oxidized by photogenerated holes at the TiO_2 electrode at its concentration of ca. 10 M, and the TiO_2 photoanode surface was damaged and became porous.[48,49] At a fairly low light intensity, the efficiency of water photoelectrolysis is normally near 100% at a well-prepared TiO_2 electrode. On the other hand, at a higher light intensity, it is reported that the photocurrent efficiency decreased.[58] Figure 10 shows the schematic correlation of the relative number of carriers at the interface of the electrode–solution junction.

8. Application of Redox Agents in the Electrochemical Photocell. For the conversion of solar energy, we have proposed the electrochemical photocell operating with a TiO_2 photoanode immersed in a basic solution and a metal counterelectrode in an acidic solution.[1,2] Here, we can propose another type of electrochemical photocell, a regenerative electrochemical photocell, converting solar to electrical energy. This can be constructed using a redox agent such as I^-/I_2 or hydroquinone/quinone which is well oxidized by photogenerated holes at TiO_2. For example, we show the current-potential curves for the case of the I^-/I_2 couple in Figure 11. The cell reactions are described as following:

at the TiO_2 photoanode

$$2I^- + 2h^+ \rightarrow I_2 \qquad (25)$$

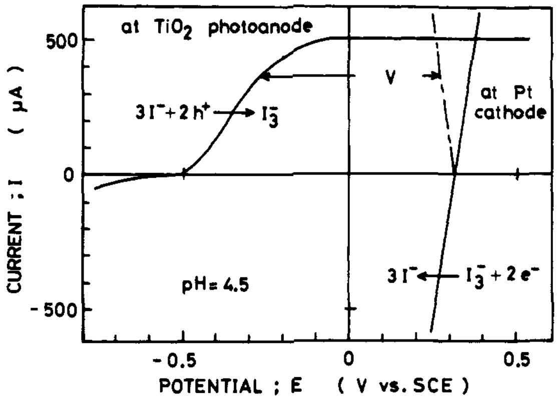

Figure 11. Current-potential curves in the regenerative electrochemical photocell of the $TiO_2/I^-/I_2/Pt$ system.

at the Pt cathode

$$I_2 + 2e^- \rightarrow 2I^- \qquad (26)$$

As for the power characteristics of this cell, the open circuit voltage becomes about 0.8 V in one solution, which surpasses that of the former type of electrochemical photocell. However, this has the disadvantage that the product (I_2) absorbs light at the absorption wavelengths of TiO_2. In order to overcome this disadvantage and realize an ideal electrochemical regenerative photocell, we feel that a more detailed search for a suitable combination of the semiconductor–redox agent system is necessary.

Conclusion

Unreduced TiO_2 is an insulator with a resistivity of ca. 10^9 Ω cm. After a reducing treatment, it can be employed for the photoanode in the electrochemical photocell which converts light energy into electrical and/or chemical energy.

In this study, we discuss the oxidation reactivity of the electroactive species at the interface of a TiO_2-solution junction, focusing upon the redox potentials of the interface species. Some crucial findings were obtained.

(1) A variety of reducing agents whose redox potentials are positioned within the TiO_2 band gap are photoelectrochemically oxidized at the TiO_2 photoanode.

(2) Competitive oxidation at the TiO_2 photoanode can be interpreted on the basis of the redox potentials of the electroactive species; that is, oxidation of a reducing agent with a more negative redox potential precedes those of others.

(3) The pH dependence of competitive oxidation can be explained based on the pH–potential relationship.

(4) The stability of the TiO_2 photoanode can be interpreted according to the prevailing competitive relationships based on the redox potentials of electroactive species.

(5) Participation of the surface states in the charge transfer can be assumed also for the competitive oxidation.

However, the concrete characteristics of the surface states have not been thoroughly elucidated and are currently under investigation in this laboratory.

References and Notes

(1) A. Fujishima and K. Honda, *Nature (London)*, **238**, 37 (1972).
(2) A. Fujishima, K. Kohayakawa, and K. Honda, *J. Electrochem. Soc.*, **122**, 1487 (1975).
(3) M. S. Wrighton, D. S. Ginley, P. T. Wolczanski, A. B. Ellis, D. L. Morse, and A. Linz, *Proc. Natl. Acad. Sci. U.S.A.*, **72**, 1518 (1975).
(4) K. L. Hardee and A. J. Bard, *J. Electrochem. Soc.*, **122**, 739 (1975).
(5) A. J. Nozik, *Nature (London)*, **257**, 383 (1975).
(6) T. Ohnishi, Y. Nakato, and H. Tsubomura, *Ber. Bunsenges. Phys. Chem.*, **79**, 523 (1975).
(7) H. Yoneyama, H. Sakamoto, and H. Tamura, *Electrochim. Acta*, **20**, 341 (1975).
(8) J. O'M Bockris and K. Uosaki, *J. Electrochem. Soc.*, **124**, 98 (1977).

(9) M. S. Wrighton, A. B. Ellis, P. T. Wolczanski, D. L. Morse, H. B. Abrahamson, and D. S. Ginley, *J. Am. Chem. Soc.*, **98,** 2774 (1976).
(10) J. G. Mavroides, J. A. Kafalas, and D. F. Kolesar, *Appl. Phys. Lett.*, **28,** 241 (1976).
(11) G. Hodes, D. Cahen, and J. Manassen, *Nature* (*London*), **260,** 312 (1976).
(12) R. H. Wilson, *J. Appl. Phys.*, **48,** 4292 (1977).
(13) A. Fujishima and K. Honda, *Seisan Kenkyu*, **22,** 478 (1970).
(14) T. Inoue, T. Watanabe, A. Fujishima, and K. Honda, *Chem. Lett.*, 1073 (1977).
(15) S. N. Frank and A. J. Bard, *J. Am. Chem. Soc.*, **99,** 303, 4667 (1977).
(16) R. N. Noufi, P. A. Kohl, S. N. Frank, and A. J. Bard, *J. Electrochem. Soc.*, **125,** 246 (1978).
(17) R. Williams, *J. Chem. Phys.*, **32,** 1505 (1960).
(18) F. Lohman, *Ber. Bunsenges. Phys. Chem.*, **87,** 428 (1960).
(19) H. Gerischer, *J. Electroanal. Chem.*, **58,** 263 (1975).
(20) A. Fujishima and K. Honda, *Denki Kagaku*, **40,** 33 (1972).
(21) A. Fujishima and K. Honda, *Seisan Kenkyu*, **22,** 524 (1970).
(22) T. Inoue, K. Kohayakawa, T. Watanabe, A. Fujishima, and K. Honda, *J. Electrochem. Soc.*, **124,** 719 (1977).
(23) A. Fujishima, E. Sugiyama, and K. Honda, *Bull. Chem. Soc. Jpn.*, **44,** 304 (1971).
(24) T. Inoue, T. Watanabe, A. Fujishima, and K. Honda, *Rev. Polarogr.*, **23,** 94 (1977).
(25) A. Fujishima, T. Inoue, T. Watanabe, and K. Honda, *Chem. Lett.*, 357 (1978).
(26) F. Sitabkhan, *Ber. Bunsenges. Phys. Chem.*, **76,** 389 (1972).
(27) A. B. Ellis, S. W. Kaiser, and M. S. Wrighton, *J. Am. Chem. Soc.*, **98,** 1635 (1976).
(28) B. Miller and A. Heller, *Nature* (*London*), **262,** 680 (1976).
(29) A. B. Ellis, S. W. Kaiser, and M. S. Wrighton, *J. Am. Chem. Soc.*, **98,** 6418 (1976).
(30) R. Memming, *J. Electrochem. Soc.*, **125,** 117 (1978).
(31) Y. Nakato, K. Abe, and H. Tsubomura, *Ber. Bunsenges. Phys. Chem.*, **80,** 1002 (1976).
(32) K. L. Hardee and A. J. Bard, *J. Electrochem. Soc.*, **124,** 215 (1977).
(33) T. Osa and M. Fujihira, *Nature* (*London*), **264,** 349 (1976).
(34) Y. Nakato, S. Tonomura, and H. Tsubomura, *Ber. Bunsenges. Phys. Chem.*, **80,** 1289 (1976).
(35) W. J. Albery and M. L. Hitchman, "Ring-Disk Electrodes", Clarendon Press, Oxford, 1970.
(36) V. G. Levich, "Physicochemical Hydrodynamics", Prentice-Hall, Englewood Cliffs, N.J., 1962.
(37) M. S. Wrighton, D. S. Ginley, P. T. Wolczanski, A. B. Ellis, D. J. Morse, and A. Linz, *Proc. Natl. Acad. Sci. U.S.A.*, **72,** 1518 (1975).
(38) M. Puorbaix, "Atlas d'Eqilibres Electrochimiques", Gauthier-Villars, Paris, 1963.
(39) A. Fujishima, A. Sakamoto, and K. Honda, *Seisan Kenkyu*, **21,** 450 (1969).
(40) T. Watanabe, A. Fujishima, and K. Hond, *Chem. Lett.*, 897 (1974).
(41) P. A. Kohl and A. J. Bard, *J. Am. Chem. Soc.*, **99,** 7531 (1977).
(42) T. Inoue, T. Watanabe, A. Fujishima, and K. Honda, *Bull. Chem. Soc. Jpn.*, **52,** 1243 (1979).
(43) H. Gerischer in "Physical Chemistry: an Advanced Treatise", Vol. 9A, H. Eyring, D. Henderson, and W. Jost, Eds., Academic Press, New York, 1970.
(44) The reorganization energy of $Fe(CN)_6{}^{4-}$ was given the value of 0.75 eV from the references: M. Gleria and R. Memming, *J. Electroanal. Chem.*, **65,** 163 (1975); F. Willig and G. Scherer, *Z. Naturforsch. A*, **31,** 981 (1976).
(45) H. Morisaki, M. Hariga, and K. Yazawa, *Appl. Phys. Lett.*, **30,** 7 (1977).
(46) A. J. Bard and M. S. Wrighton, *J. Electrochem. Soc.*, **124,** 1706 (1977).
(47) H. Gerischer, *J. Electroanal. Chem.*, **82,** 133 (1977).
(48) K. Kohayakawa, T. Yamabe, A. Fujishima, and K. Honda, *Nippon Kagaku Kaishi*, 1351 (1978).
(49) L. A. Harris, D. R. Cross, and M. E. Gerstner, *J. Electrochem. Soc.*, **124,** 839 (1977).
(50) J. H. Carey and B. G. Oliver, *Nature* (*London*), **259,** 554 (1976).

High-Pressure Kinetic Evidence for an Associative–Dissociative Changeover for Solvent Exchange Mechanism on the Divalent Metal Ions along the First-Row Transition Metals[1]

Felix K. Meyer, Kenneth E. Newman, and André E. Merbach*

Contribution from the Institut de Chimie Minérale et Analytique, Université de Lausanne, 3, Place du Château, CH-1005 Lausanne, Switzerland. *Received February 9, 1979*

Abstract: The effect of pressure (up to 200 MPa) on the methanol exchange on $[Mn(CH_3OH)_6](ClO_4)_2$ and $[Fe(CH_3OH)_6](ClO_4)_2$ has been studied utilizing ^1H FT NMR T_2 measurements. The derived volumes of activation, ΔV^* in $cm^3\ mol^{-1}$, together with the previously published values for methanol exchange on cobalt(II) and nickel(II) (-5.0 ± 0.2 (Mn^{2+}), $+0.4 \pm 0.3$ (Fe^{2+}), $+8.9 \pm 0.3$ (Co^{2+}), and $+11.4 \pm 0.6$ (Ni^{2+})), give evidence for an associative-dissociative mechanistic changeover for solvent exchange along the first-row transition metals. This is in disagreement with the general belief that substitution reactions on all divalent ions occur via a dissociative activation mode.

Introduction

Simple substitution reactions on divalent cations of the first-row transition metals are generally thought to have a dissociative activation mode. Such a behavior has been clearly established by Eigen and Wilkins for complex formation reactions on Ni(II) and has then been further extended to the other divalent metal ions.[3,4] The exchange of solvent molecules between the primary solvation shell of a cation and bulk solvent may therefore be considered a fundamental reaction for metal ions in solutions. Since one cannot vary the concentration of free solvent nor change the nature of the incoming "ligand", clues to establish the mechanism of solvent exchange are given mainly by the activation parameters. Unfortunately, activation enthalpies and entropies obtained from NMR studies are prone to large nonrandom errors, particularly for paramagnetic ions.[5,6] Even though studying the variation of rates with pressure is technically difficult, the volume of activation, ΔV^*,

$$\Delta V^* = -RT\left(\frac{\partial \ln k}{\partial P}\right)_T \tag{1}$$

has proved to be extremely useful in the diagnosis of reaction mechanisms.[7,8] It has been observed that random and nonrandom errors in the determination of the rate constants affect ΔV^* less than ΔS^* when similar experimental approaches are used.[6,9] If, as for solvent exchange, there is no charge separation or cancellation on going from the reactants to the transition state, a positive ΔV^* can be directly related to a dissociative activation mode and a negative ΔV^* to an associative process.[10]

We have applied high-pressure NMR to investigate nonaqueous solvent exchange. In a previous paper[10] we reported volumes of activation for *N*,*N*-dimethylformamide, acetoni-

0002-7863/79/1501-5588$01.00/0